EVOLUTION IN ELECTRICAL AND ELECTRONIC ENGINEERING
e-ISSN: 2756-8458

EEEE

Vol. 6 No. 2 (2025) 329-338
https://publisher.uthm.edu.my/periodicals/index.php/eeee

Rotor Pole Analysis of Various 3 Phase Outer Rotor Hybrid Excitation Flux Switching Motor

Nurhazwani Hadhirah Shamsul[1], Erwan Sulaiman[1]*

[1] *Department of Electrical Engineering, Faculty of Electrical and Electronic Engineering, Universiti Tun Hussein Onn Malaysia, 86400, Batu Pahat, Johor, MALAYSIA*

*Corresponding Author: erwan@uthm.edu.my
DOI: https://doi.org/10.30880/eeee.2025.06.02.040

Article Info

Received: 20 June 2025
Accepted: 18 August 2025
Available online: 30 October 2025

Keywords

Outer Rotor Hybrid Excitation Flux Switching Motor, Cogging Torque, Chamfering, Notching, Pole Pairing.

Abstract

Hybrid Excitation Flux Switching Machine (HEFSM) represent an emerging class of electric machines that integrate both permanent magnets and field windings within the stator, enabling a controllable flux mechanism. Several benefits of this special topology include high power density, efficiency, and wide-band operation. However, the choice of rotor-pole configurations has a big impact on how well HEFSMs work since they control the machine's electromagnetic properties such torque generation, efficiency, cogging torque, and operational stability. Their employment in vital fields including robotics, electric vehicles (EVs), and renewable energy systems is restricted by issues like excessive cogging torque, torque ripple, and magnetic losses, despite their potential. This study aims to analyze and evaluate the impact of various rotor-pole combinations on the electromagnetic performance of 3-phase OR-HEFSMs. JMAG Designer is utilized to simulate and compare the electromagnetic behavior of multiple configurations, focusing on key parameters such as torque output, cogging torque, and flux linkage. The analysis explores the influence of both integer and fractional rotor-pole combinations, providing insights into their advantages and trade-offs. Furthermore, this research investigates techniques to reduce cogging torque, a primary source of torque ripples and noise in FSMs. Structural techniques such as chamfering, notching, and pole pairing were implemented, yielding critical design insights into rotor pole optimization for OR-HEFSMs. These findings support the future development of high-performance machines for electric mobility and renewable energy applications.

1. Introduction

Several studies have divided flux switching motor (FSMs) into three primary classes according on the source of its excitation, Permanent Magnet Flux Switching Motor (PM-FSM), Field Excitation Motor (FE-FSM) or Wound Field and Hybrid Excitation Motor (HE-FSM). Despite the advantages offered by FSM, they have certain drawbacks, including notable cogging torque and ripples, resulting in noticeable vibrations [1]. The HE-FSM combines two excitation sources—permanent magnets (PMs) and field excitation windings (FEWs)—in a unique configuration that allows for greater control over the motor's magnetic field. This dual-source excitation offers significant advantages, including improved torque control, power density, and the capability to sustain high performance across diverse speeds and loads [2]. An outer rotor configuration further amplifies the potential of the HE-FSM by

positioning the rotor outside the stator. Unlike traditional inner rotor motors, this structural adjustment provides multiple advantages: high torque density, improved efficiency and reduced cogging [3]. It also offers superior cooling due and enhances thermal performance [4]. Additionally, rotor-pole configurations significantly influence the torque production and ripple, flux distribution and core losses and cogging torque of these motors. There has been a strict requirement to reduce cogging torque in terms of increasing output efficiency and reducing vibration and noise for a long time [5]. However, despite their potential, comprehensive studies on the slot-pole effects in outer rotor HE-FSMs remain underexplored. This study aims to address these challenges by systematically analyzing the electromagnetic performance of various rotor-pole configurations focusing on identifying the most optimal configuration and implementing strategies to reduce cogging torque to ensure smoother operation and enhanced motor performance.

The performance of outer rotor HEFSMs is heavily influenced by their rotor-pole configurations, which impact on critical factors like torque production, torque ripple, flux distribution, and electromagnetic efficiency. The specific combination of stator slots and rotor poles determines the cogging torque frequency. Poor rotor-pole combinations can lead to higher cogging torque. Additionally, cogging torque, a common issue caused by the interaction of the rotor's permanent magnets with the stator slots, can lead to vibration, noise, and reduced motor smoothness, further affecting motor performance. Even when there is no current flowing through the windings, this magnetic attraction causes periodic torque changes as the rotor rotates. A high cogging torque may have a negative impact on the motor's output torque. As a result, the motor's performance could be impacted from low output torque. Low output power is caused by low output torque. When the cogging torque reduction approach is used to the design, the outcomes will vary.

2. Literature Review

2.1 Inner and Outer Rotor Hybrid Excitation Flux Switching Motor Configuration

The main difference between inner and outer rotor motors is the placement of the rotor relative to the stator in which when the rotor is inside the motor, while the stator is on the outside is known as inner rotor motors while outer rotor motors are vice versa. Inner rotor motors have a lower moment of inertia compared to outer rotor motors, which translate into higher acceleration, faster response, and a lower mechanical time constant. In outer rotor motors, the material selection and weight reduction features are critical to reducing the moment of inertia. The operating principle of OR-HEFSM is illustrated in Fig. 1.

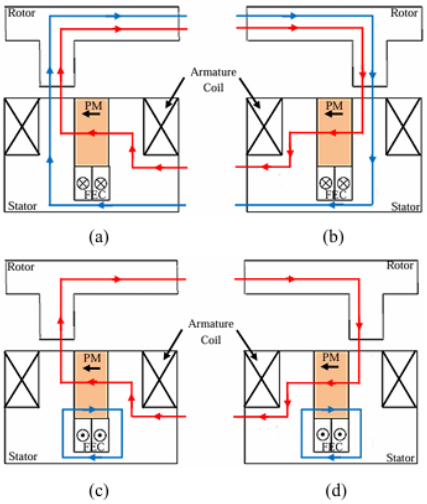

Fig. 1 *Operating Principle of OR-HEFSM (a) θe = 0° (b) θe = 180° More Excitation, (c) θe = 0° (b) θe = 180° Less Excitation.*

2.2 Review of Cogging Torque Reduction Technique in Flux Switching Motor

Torque production in FSM relies on controlling the flux path within the machine by switching the magnetic field between different rotor poles [6]. A fluctuating magnetic field is produced in the air gap by this control over the magnetic flow. The air-gap field harmonics, including the fundamental component responsible for the primary torque generation and higher harmonics owing to the structure of the rotor, play a crucial role [7]. The effects of torque ripples transcend in the form of vibration, acoustic noise, and structural resonance which are transferred from the source to the load via rotor shaft. Therefore, the cogging torque reduction technique will reduce the cogging torque and torque ripples. The cogging torque reduction technique can be done through motor drives or

Evolution in Electrical and Electronic Engineering Vol. 6 No. 2 (2025) p. 329-338

geometrical modifications [8]-[9]. In general, cogging torque reduction for design methods can be accomplished by two aspects which include modifications on the rotor and the stator side. Modification on the rotor side has been widely used compared with the stator part as it complicates the stator manufacturing and consequently increases the manufacturing cost of the machine. The geometrical modification to reduce the cogging torque in this study is divided into several techniques which are pole pairing, chamfering and notching. While these methods have been widely studied in conventional PM and switched reluctance machines, their combined and comparative application specifically in OR-HEFSMs is less explored. The project conducts a fair comparison of the three reduction techniques under identical simulation conditions that provides a consistent benchmark for evaluating the effectiveness of each method, which is often lacking in fragmented literature studies that use differing models or parameters.

3. Methodology

This section presents the flow and process of the project, including a thorough explanation. The implementation of this project is divided into three parts, design, analysis and cogging torque reduction. The number of poles for this project differ for each design, using 8, 10, 14, 16 respectively for a three-phase motor. The number of rotor pole and stator slot combination can be expressed using Equation (1).

$$N_r = N_s\left(1 \pm \frac{k}{2q}\right) \tag{1}$$

3.1 System Flowchart of Overall Project

Fig. 2 illustrates the step-by-step process for designing, analysing and cogging torque reduction techniques. For this project, JMAG-Designer version 18.1 is used to design the motor. It begins with drawing the parts and region radial pattern followed by setting of material use, condition, circuit, and mesh. After the confirmation of operating principle, various characteristics of the three-phase OR-HFSM are investigated which include no load and load analysis of the proposed motor. The performance analysis of various rotor pole numbers is measured at open and short circuit conditions. Then, based on the successful designs at the design stage, one of the most optimal designs will undergo the cogging torque reduction techniques to refine the cogging torque of the OR-HEFSM. This method also compares the effectiveness of three cogging torque reduction techniques which are chamfering, notching, and pole pairing.

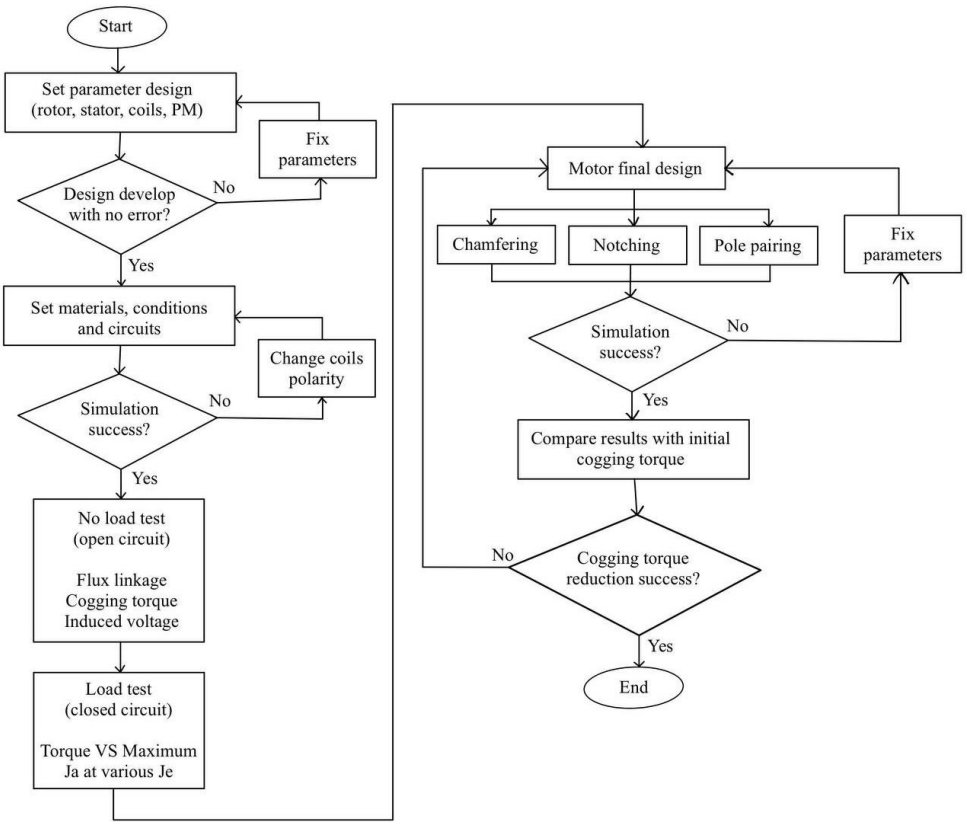

Fig. 2 *Overall implementation of the study*

4. Result and Analysis

This section discusses the results and comparison from the analysis conducted in this project. Once the parameters have been clearly determined and set in the motor, all four of the designs of ORHEFSM will be analyzed based on 2D-FEA for no load analysis and load analysis. Fig. 3 shows the illustration design of all four different configurations of OR-HEFSM in Geometry Editor.

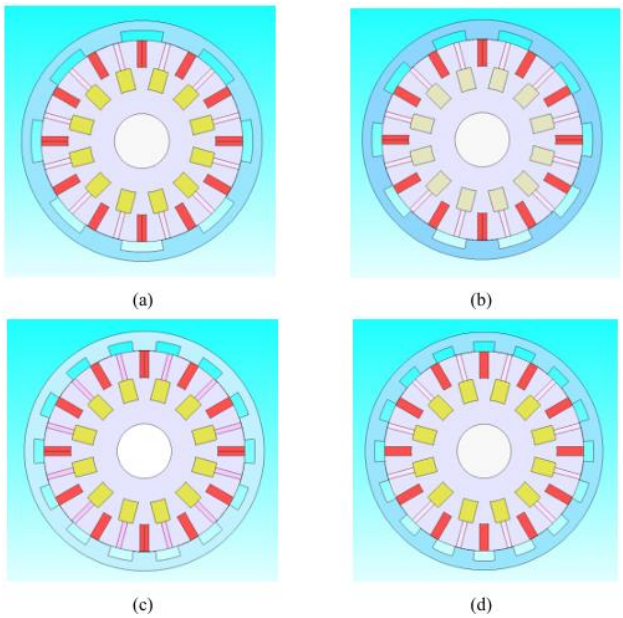

Fig. 3 *Complete design of (a) 12S-8P OR-HEFSM, (b) 12S-10P OR-HEFSM, (c) 12S-14P OR-HEFSM and (d) 12S-16P OR-HEFSM*

4.1 No Load Analysis

The analysis of flux linkage, induced voltage, cogging torque and torque vs Ja at maximum armature coil current density for the various design topologies is conducted in this section at open circuit condition. For flux linkage analysis, the 12S-8P has a significant flux linkage of 0.012 Wb when compared to other outer rotor PMFSM configurations, as illustrated in Fig. 4.

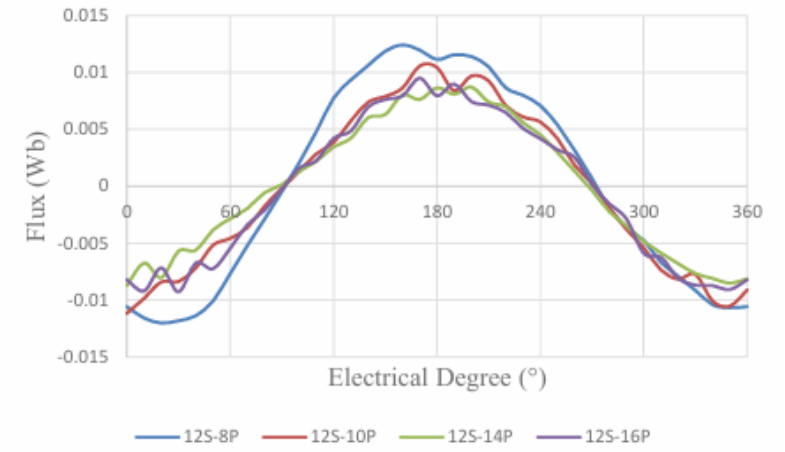

Fig. 4 U-*phase flux linkage of the 4 designs of OR-HEFSM*

The back electromotive force (back-EMF) analysis is to study the induced voltage. The back-EMF generated from field excitation coil with the speed of 1200 rpm for different pole numbers are illustrated in Fig. 5. 12S-16P OR-HEFSM has the highest positive amplitude of 97V, the least back EMF (F) is 12S-8P at 48V.

Evolution in Electrical and Electronic Engineering Vol. 6 No. 2 (2025) p. 329-338

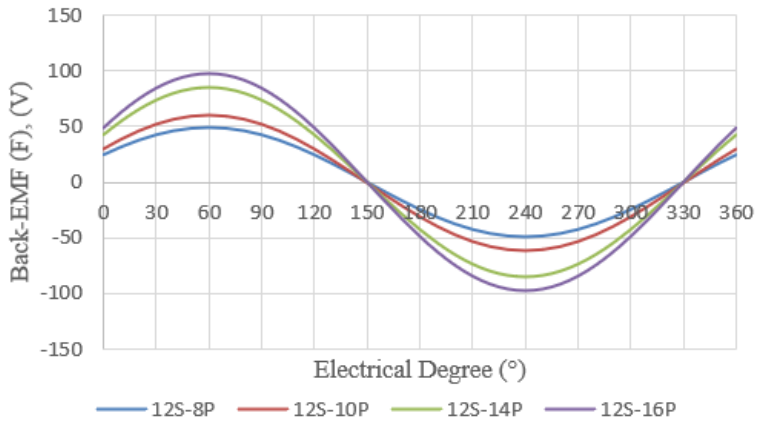

Fig. 5 *Back-EMF of the 4 designs of OR-HEFSM*

Fig. 6 shows the cogging torque characteristics of various rotor pole topologies with 12S-10P having the lowest cogging torque followed by 12S-14P, 12S-8P and 12S-16P, with a peak-to-peak value of approximately 540 Nm, 546 Nm, 558 Nm and 634 Nm.

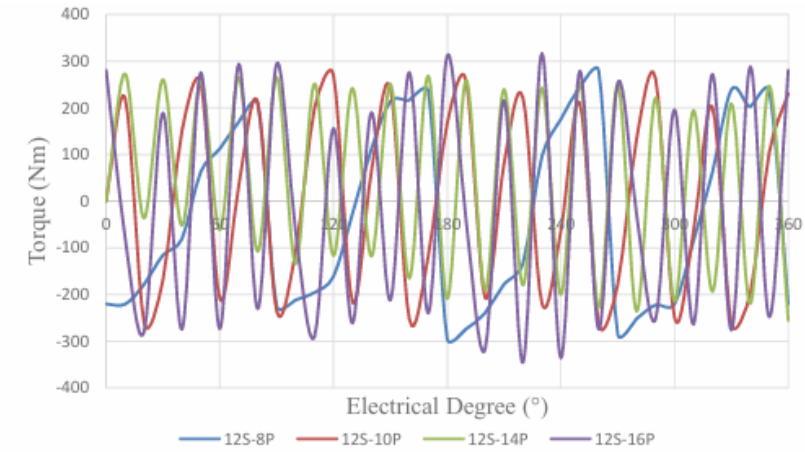

Fig. 6 *Cogging torque of the 4 designs of OR-HEFSM*

The performance of an electric motor at the maximum current density, Ja, is what determines its capabilities. Fig. 7 illustrates the torque versus Ja for the four designs. The influence on torque is examined when the Ja is changed from 5 Arms/mm^2 to 30 Arms/mm^2. As the value of Ja grows, it is observed that the torque increases. The minimum torque is produced by 12S-16P with 32.25 Nm.

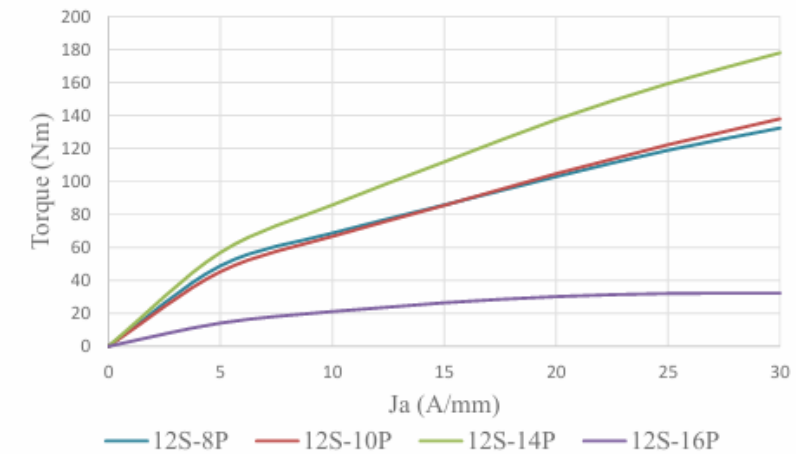

Fig. 7 *Torque versus Ja at Maximum Armature Coil Density of the 4 designs of OR-HEFSM*

Table 1 shows the performance comparison of the various rotor pole numbers. It can be concluded from the table that topology 12S-10P is the most optimal topology compared to other topologies for OR-HEFSM as it has low cogging torque, and back EMF but notably high torque with high flux linkage.

Table 1 *No load performance comparison of various rotor pole topologies*

Analysis	12S-8P	12S-10P	12S-14P	12S-16P
3 Coil Test (Wb)	0.0124	0.0106	0.0087	0.0095
Back-EMF (V)	48.60	60.75	85.05	97.21
Cogging Torque (Nm)	558.39	539.51	546.01	633.51
Torque at J_A= 30 A/mm (Nm)	132.36	137.93	177.94	32.25

4.2 Load Analysis

Motor performance was examined under closed-circuit conditions with armature current densities, JA ranging from 0 Arms/mm^2 up to 30 Arms/mm^2. This condition involved analyzing the output torque of several motor topologies against different field excitation current densities, Je. Results were sketched from Fig. 8 until Fig. 11 for four different rotor configurations. In 12S-8P OR-HEFSM, from Fig. 8 the maximum torque of 115.51Nm was obtained by the model when the armature current density was set to 15 Arms/mm^2 and reduced until 30 Arms/mm^2. The torque achieved at different field excitation current densities from 5 Arms/mm^2 to 30 Arms/mm^2 are 45 Nm, 92 Nm, 116 Nm, 109 Nm, 102 Nm, and 97 Nm respectively.

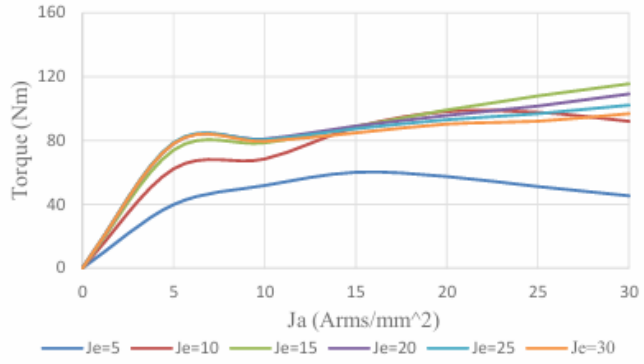

Fig. 8 *Torque vs Ja at various Je of 12S-8P OR-HEFSM*

In Fig. 9, the higher the amount of armature current density, Ja, the higher the torque would be generated. The detailed torque of the motor at different field excitation current densities from 5 Arms/mm^2 to 30 Arms/mm^2 are 48 Nm, 93 Nm, 129 Nm, 146 Nm, 152 Nm and 155 Nm respectively. The maximum torque of 155.41 Nm was obtained by the model when both Ja and Je were set to 30 Arms/mm^2.

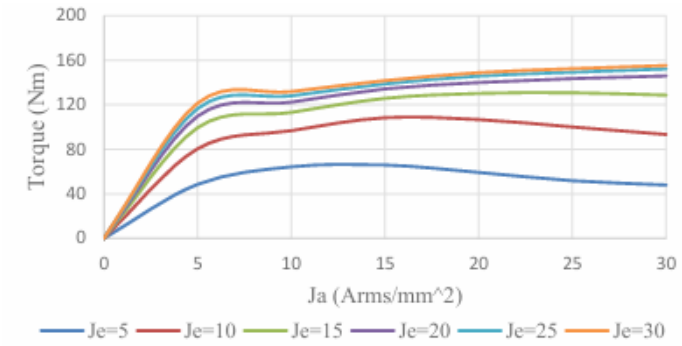

Fig. 9 *Torque vs Ja at various Je of 12S-10P OR-HEFSM*

Evolution in Electrical and Electronic Engineering Vol. 6 No. 2 (2025) p. 329-338

In Fig. 10, the maximum torque of 240.62 Nm was obtained by the model when the armature current density was set to 30 Arms/mm², but the increment stopped at Ja 20 Arms/mm² and slowly reduced the optimal point. The torque achieved at different field excitation current densities from 5 Arms/mm² to 30 Arms/mm² are 61 Nm, 119 Nm, 171 Nm, 204 Nm, 225 Nm, and 241 Nm respectively.

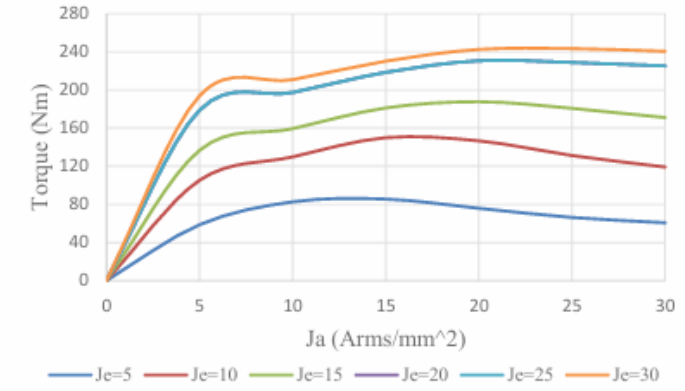

Fig. 10 *Torque vs Ja at various JE of 12S-14P OR-HEFSM*

Fig. 11 shows that 12S-16P topology has the lowest cogging torque value but does not have the best slot and rotor pole combination as the cogging torque increases halfway then reduces. The 12S-16P configuration offers more uniform airgap flux density due to better alignment between stator teeth and rotor poles that results in smoother magnetic transitions which reduces the abrupt changes in reluctance that causes low torque. The detailed torque of the motor at different field excitation current densities from 5 Arms/mm² to 30 Arms/mm² are 2 Nm, 5 Nm, 11 Nm, 14 Nm, 13 Nm and 16 Nm respectively.

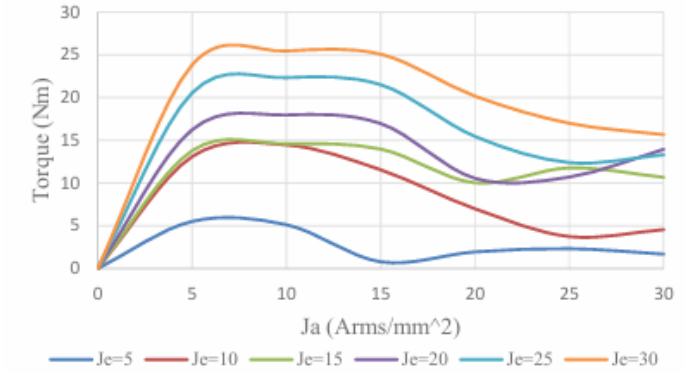

Fig. 11 *Torque vs Ja at various Je of 12S-16P OR-HEFSM*

Table 2 shows the performance comparison of the various rotor pole design for load analysis. It can be concluded from the table that topology 12S-10P is the most suitable topology for OR-HEFSM as the armature current density increased with the field excitation current density, higher than Ja achieved the optimal point later compared to lower Je.

Table 2 *Performance comparison of various rotor pole topologies for load test.*

Analysis	12S-8P	12S-10P	12S-14P	12S-16P
Torque (Nm)	115.51	155.41	240.62	15.67

4.3 Cogging Torque Reduction

The analysis of cogging torque reduction for the proposed 12S-10P OR-HESFSM topology is conducted in this section using three different techniques which are chamfering, notching and pole pairing. Fig. 12 shows the illustration motor design when the techniques are applied.

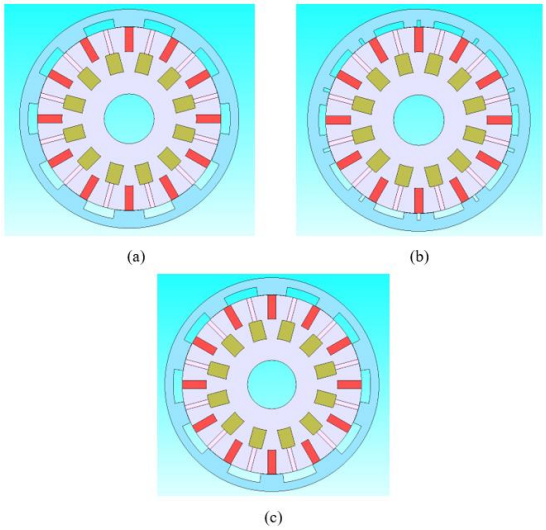

Fig. 12 *Motor design for cogging torque reduction (a) chamfering method, (b) notching method and (c) pole pairing method.*

Based on the motor design of 12S-10P OR-HEFSM, the chamfering technique is adopted. Curve chamfer dimension is measured by the curve radius of the chamfer located on the tip of the rotor pole. The chamfer is applied on both tips on each rotor pole. The cogging torque resulting from the chamfering method exhibited different behaviors as illustrated in Fig. 13 showing the peak-to-peak cogging torque values and average output torque. The most optimal cogging torque reduction happens at an arc angle of 10˚ at 359.6 Nm peak-to-peak and achieved 33.35% cogging torque reduction from the initial value.

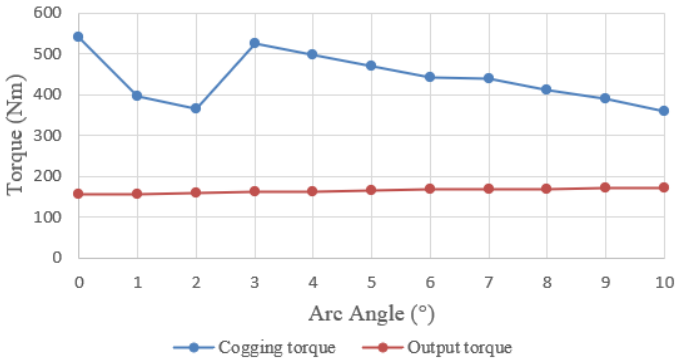

Fig. 13 *Cogging torque reduction chamfering method*

The influence of parameters, which is the depth of a notch on the cogging torque and output torque is investigated as shown in Fig. 14. The analysis of designs differs with a notch depth from 1 mm to 10 mm showing a decrement of peak-to-peak cogging torque value with an increasement of notch depth. The lowest cogging torque reduction value is achieved at a notch depth of 8mm with 450.94 Nm with 16.42% cogging torque reduction from the initial design.

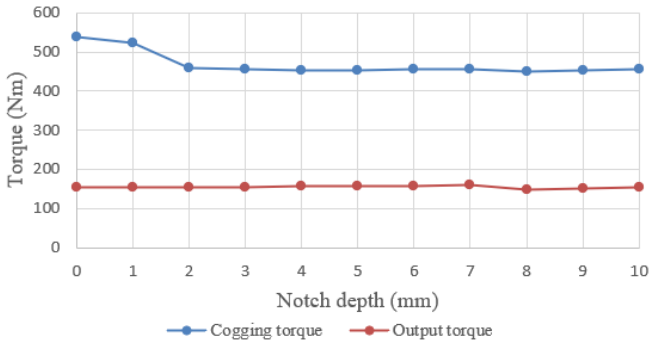

Fig. 14 *Cogging torque reduction notching method*

Fig. 15 shows the result of three different rotor configuration for pole pairing technique. This cogging torque reduction approach uses a pole pairing method that involves geometrically matching two rotor pole widths. Because the 12S-10P has an even number of rotor poles, the manipulative pole and the pole whose width is maintained at its initial width will alternate. Design 2 with a peak-to-peak cogging torque value of 101.28 Nm achieved the lowest value with 81.23% of cogging torque reduction from the initial design.

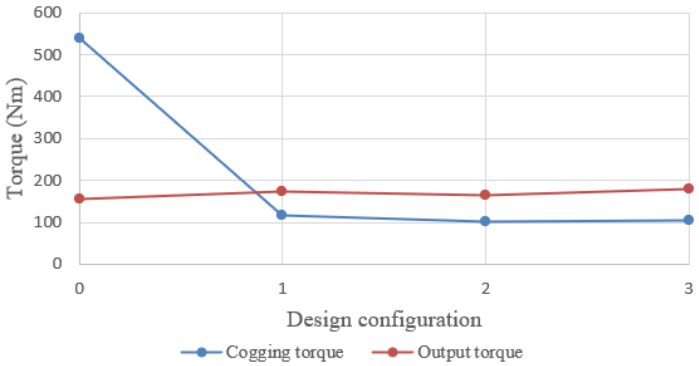

Fig. 15 *Cogging torque reduction pole pairing method*

Table 3 shows the performance comparison of the cogging torque reduction techniques applied. It can be concluded that the most suitable method to achieve the lowest cogging torque produced is by applying the pole pairing method as it relies on electromagnetic symmetry and phase-shifting between pole pairs to suppress cogging harmonics. This method effectively distributes the magnetic flux in a more balanced manner, reducing the airgap flux density fluctuation. The cogging torque is cut down from 539.51 Nm to 101.28 Nm with a percentage reduction of 81.23% showing the most percentage reduction compared to the other two methods while the output torque increased a little by 10.46 Nm from 155.41 Nm to 165.87 Nm.

Table 3 *Overall performance on applied cogging torque reduction methods*

Method	Cogging torque (Nm)	Maximum torque (Nm)	Percentage reduction (%)
Chamfering	359.6	158.21	33.35
Notching	450.94	148.93	16.42
Pole pairing	101.28	165.87	81.23

5. Conclusion

The rotor pole analysis of various 3 phase outer rotor HEFSM designs have been investigated. Initial results of the topologies were analyzed based on 2D-FEA using the JMAG software. There are 4 topologies being analyzed. Based on the no-load and load analysis, 12S-10P OR-HEFSM has achieved better performance characteristics compared to other topologies. The analyzed result achieved cogging torque of 539.51 Nm peak-to-peak, induced back-emf of 60.75 V and average torque of 137.93 Nm. Then with the most optimal configuration, cogging torque reduction methods have been investigated on 12S-10P OR-HEFSM. The reduction technique adopted was the classical techniques such as chamfering, notching and pole pairing. It can be observed that the pole pairing technique is substantial to reduce cogging torque but also preserves overall motor performance. These techniques provided a significant decrease in the cogging torque which fulfills the objective.

Acknowledgement

The authors would also like to thank the Faculty of Electrical and Electronic Engineering, Universiti Tun Hussein Onn Malaysia for its support. Their guidance and assistance have been instrumental in the successful completion of this endeavor.

Conflict of Interest

Authors declare that there is no conflict of interests regarding the publication of the paper.

Author Contribution

The authors confirm contribution to the paper as follows: ***study conception and design:*** *Nurhazwani Hadhirah Shamsul, Erwan Sulaiman;* ***data collection:*** *Nurhazwani Hadhirah Shamsul;* ***analysis and interpretation of results:*** *Nurhazwani Hadhirah Shamsul, Erwan Sulaiman;* ***draft manuscript preparation:*** *Nurhazwani Hadhirah Shamsul, Erwan Sulaiman. All authors reviewed the results and approved the final version of the manuscript.*

References

[1] Abunike, E.C. & Okoro, O.I. & Far, Aliakbar & Aphale, Sumeet S.. (2023). Advancements in Flux Switching Machine Optimization: Applications and Future Prospects. IEEE Access. PP. 1-1. 10.1109/ACCESS.2023.3321862.

[2] Mörée, G., & Leijon, M. (2022). Overview of Hybrid Excitation in Electrical Machines. Energies, 15(19), 7254.

[3] M. Z. Ahmad, E. Sulaiman, and T. Kosaka, ‘‘Optimization of outer-rotor hybrid excitation fsm for in-wheel direct drive electric vehicle,’’ in 2015 IEEE International Conference on Mechatronics (ICM), 2015, pp. 691–696.

[4] S. Akbar, F. Khan, W. Ullah, B. Ullah, A. H. Milyani, and A. A. Azhari, ‘‘Performance analysis and optimization of a novel outer ro-tor field-excited flux-switching machine with combined semi-closed and open slots stator,’’ Energies, vol. 15, no. 20, p. 7531, 2022.

[5] IEEJ,“ High perforance of small motor, ”IEEJ Technical Repoort, Vol. 744, 1999.

[6] C. E. Abunike, O. I. Okoro, A. J. Far and S. S. Aphale, "Advancements in Flux Switching Machine Optimization: Applications and Future Prospects," in IEEE Access, vol. 11, pp. 110910-110942, 2023.

[7] N. Fernando, I. U. Nutkani, S. Saha and M. Niakinezhad, "Flux switching machines: A review on design and applications," 2017 20th International Conference on Electrical Machines and Systems (ICEMS), Sydney, NSW, Australia, 2017, pp. 1-6.

[8] K. Wang, Z. Q. Zhu, and G. Ombach, “Torque improvement of five-phase surface-mounted permanent magnet machine using third-order harmonic,” IEEE Trans. Energy Convers., vol. 29, no. 3, pp. 735–747, 2014.

[9] L. Hao, M. Lin, D. Xu, W. Zhang, and N. Li, “Rotor design techniques for reducing the cogging torque in a novel dual-rotor axial field flux-switching permanent magnet machine,” in 2014 17th International Conference on Electrical Machines and Systems (ICEMS), 2014, pp. 1581–1586.